

See discussions, stats, and author profiles for this publication at: <https://www.researchgate.net/publication/231713264>

On the Structural and Stability Features of Linear Atomic Suspended Chains Formed from Gold Nanowires Stretching

ARTICLE *in* NANO LETTERS · JUNE 2004

Impact Factor: 13.59 · DOI: 10.1021/nl049725h

CITATIONS

78

READS

45

8 AUTHORS, INCLUDING:



Varlei Rodrigues

University of Campinas

37 PUBLICATIONS 1,415 CITATIONS

SEE PROFILE



Sócrates O Dantas

Federal University of Juiz de Fora

52 PUBLICATIONS 1,791 CITATIONS

SEE PROFILE



Daniel Ugarte

University of Campinas

135 PUBLICATIONS 9,447 CITATIONS

SEE PROFILE



Douglas S. Galvao

University of Campinas

258 PUBLICATIONS 3,901 CITATIONS

SEE PROFILE

On the Structural and Stability Features of Linear Atomic Suspended Chains Formed from Gold Nanowires Stretching

Pablo Z. Coura,[†] Sergio B. Legoas,[‡] Anderson S. Moreira,[§] Fernando Sato,^{||}
Varlei Rodrigues,[⊥] Sócrates O. Dantas,^{*,†} Daniel Ugarte,^{||,⊥} and
Douglas S. Galvão^{||}

*Departamento de Física, ICE, Universidade Federal de Juiz de Fora,
36036-330 Juiz de Fora MG, Brazil, Departamento de Física, Universidade Federal
do Amazonas, 69077-000 Manaus AM, Brazil, Centro Brasileiro de Pesquisas Físicas,
Rua Xavier Sigaud 150, 22290-180 Rio de Janeiro RJ, Brazil, Instituto de Física Gleb
Wataghin, Universidade Estadual de Campinas, 13083-970 Campinas SP, Brazil, and
Laboratório Nacional de Luz Sincrotron, 13084-971 Campinas SP, Brazil*

Received February 19, 2004; Revised Manuscript Received April 20, 2004

ABSTRACT

Metallic nanowires (NWs) have been intensely investigated in the past years, but details on their formation are still not completely understood. In this work we report high resolution transmission electron microscopy data and molecular dynamics simulation results for gold NW elongation. Our results show that different initial crystallographic orientations lead to very differentiated linear atomic suspended chain (LAC) formations and strongly support that kinetic aspects are the dominant mechanisms determining the LAC morphologies.

A considerable effort has been devoted to understanding the structural and conductance properties of metallic nanowires (NWs) and suspended chains at the nanoscale.^{1–8} The renewed interest in these nanosized systems is in part due to the observation of new phenomena (quantized conductance, etc.) and to the new potential technological applications (molecular electronics, etc.). From an experimental point of view, two techniques have been mostly used: mechanically controllable break junction^{3,8,9} and in situ high-resolution transmission electron microscopy (HRTEM).^{5,8,12–14} The former is more appropriate for conductance experiments while the latter allows real time visualization, providing a better evaluation of the dynamical atomistic aspects of NW elongation.

To understand the mechanical and electronic behaviors of metallic nanowires, many theoretical studies have been carried out using different approaches, such as atomistic,^{2,15–18} continuous,^{19,20} or mixed model simulations applying empirical or post-empirical potential,^{21–23} and even first-principles quantum mechanics calculations.^{24–28} Despite the enormous

amount of theoretical work on these systems and the important knowledge gained from those simulations, some fundamental aspects on the mechanism of formation and structural stability of NWs remain unclear, and there is a need for further studies. Among the limitations of some of the present methodologies, we can mention high computational cost, artificial periodic boundary conditions, unrealistic pulling velocity, and difficulties to incorporate the experimentally observed fact that different crystallographic directions produce distinct results.^{8,29} Moreover, no systematic analyses for different crystallographic orientations have been carried out for these systems that take into account the statistical aspects of the experimental conditions (temperature fluctuations, grain size, boundaries, and morphology, etc.).

In this letter, we report both experimental HRTEM and theoretical studies on the elongation of gold nanowires and the mechanism leading to the formation of linear suspended gold atom chains, using the calculations to address the NW dynamic evolution.

Experimentally, gold nanowires are generated in situ in a HRTEM (JEM 3010 URP, 300 kV, 0.17 nm resolution, at LME/LNLS Campinas, Brazil) using the method developed by Takayanagi's group.¹⁰ The microscope electron beam (current density 100 A/cm²) is focused on a self-supported polycrystalline gold thin film (5 nm thick, deposited on a holey carbon grid) to drill holes at different sites until

* Corresponding author. E-mail: dantas@fisica.ufjf.br. Tel: +55-32-3229-3307. Fax: +55-32-3229-3312.

[†] Universidade Federal de Juiz de Fora.

[‡] Universidade Federal do Amazonas.

[§] Centro Brasileiro de Pesquisas Físicas.

^{||} Universidade Estadual de Campinas.

[⊥] Laboratório Nacional de Luz Sincrotron.

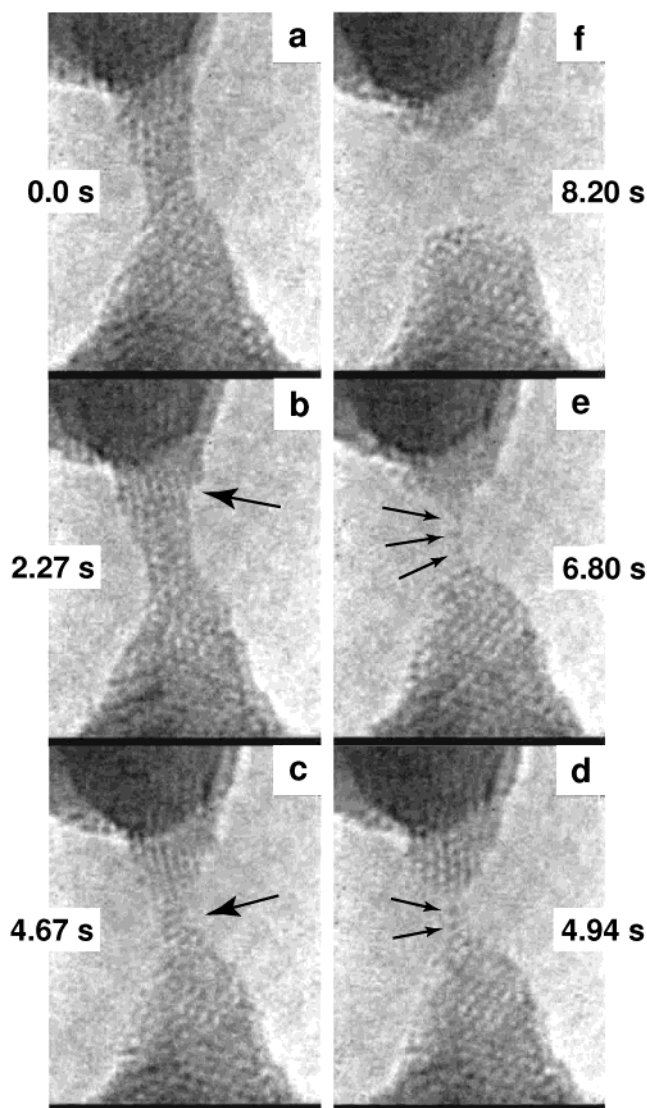


Figure 1. HRTEM images of [100] gold nanowire time evolution. A linear chain with two atoms is formed in (d), and in (e) the number of gold atoms has increased to three (indicated by arrows) before breaking (f). See text for discussions.

nanometric bridges (or NWs) are formed between neighboring holes. To perform the atomic resolution image acquisition, the electron beam intensity is reduced to ~ 30 A/cm² (see Supporting Information, video 1). Subsequently, the bridges spontaneously elongate and finally break due to relatively slow movements of the apexes. A high sensitivity TV camera (Gatan 622SC, 30 frames/s) was used to record NW real-time evolution.

In Figure 1 we present a sequence of snapshots of the formation of linear atomic suspended gold chains (LACs). NWs elongate spontaneously and become thinner (Figure 1c); in some cases the apexes slide (Figure 1b). Before the NW rupture linear chains can be formed whose lengths are in the 2–4 atoms range (Figures 1d and 1e), these linear chains may last several seconds before breaking (Figure 1d) and then the apexes retract (Figure 1f). The whole dynamical process can be better visualized in the movie of the experimental realization (Supporting Information, video 2).

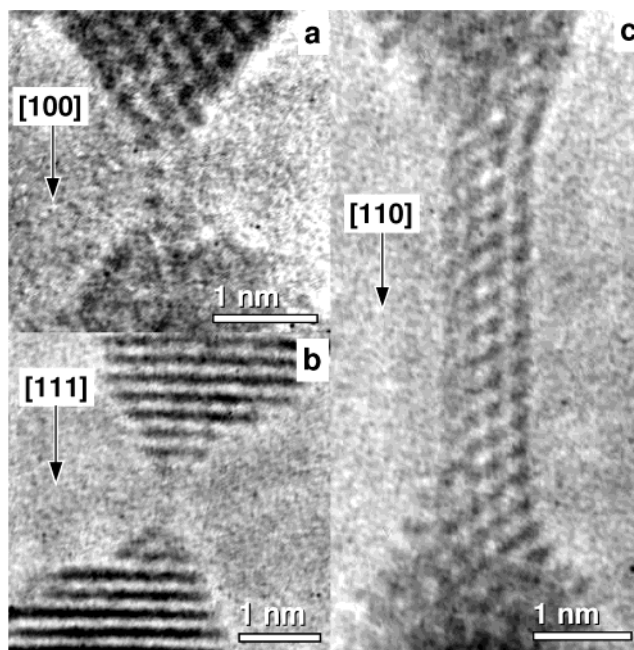


Figure 2. HRTEM images of gold nanowire formation for different crystallographic directions.

A whole analysis of linear atomic chain formation in gold has been previously reported in ref 12.

The structural and dynamic features are quite different depending on the crystallographic orientation of the NW elongation direction (Figure 2 and videos 3–5, SI). Just before rupture, gold NWs are crystalline and free of defects; in particular, they assume only three kinds of atomic arrangements, where the NW structure adjusts such that one of the [111]/[100]/[110] gold zone axes lies approximately parallel to the elongation direction.⁸ One example of each kind of NW is shown in Figure 2. In addition, using time-resolved HRTEM, we have observed that [111] and [100] NWs form biconical constrictions with ductile behavior, allowing the evolution to one-atom-thick contact (see Figure 2a and 2b). On the other hand, [110] NWs display rod-like morphology (see Figure 2c) and break abruptly when they are rather thick (3–4 atoms), alike a brittle material. The effect of elongation direction on the morphology, structure, and conductance has already been thoroughly analyzed in refs 8 and 23.

To theoretically address the wire elongation dynamics, it is necessary to have a realistic description of the experimentally generated NWs. To do so, systems with thousands of atoms should be considered, which precludes the use of *ab initio* or even semiempirical quantum methods. For this purpose, we have developed a methodology based on tight-binding molecular dynamics (TB-MD)³⁰ techniques using second-moment approximation (SMA)³¹ with a small set of adjustable parameters. This approach is based on the well-known fact that cohesive properties of transition metals and their alloys originate mainly from the large *d*-band density of states (DOS). Also, thermodynamic and structural quantities have been shown to be insensitive to the DOS details.³² These magnitudes are dominated by the electronic bandwidth. This TB–SMA molecular dynamics approach has proved

to be very effective on the study of face centered cubic (fcc) and body centered cubic (bcc) structures and alloys,³³ as well as to analyze the diffusion of clusters and particles on metal surfaces.³⁴ The cohesive energy E_c of the system can be obtained by

$$E_c = \sum_i [\sum_j D_1 e^{-p(r_{ij}/r_0-1)} - \{\sum_j D_2^2 e^{-2q(r_{ij}/r_0-1)}\}^{1/2}]$$

where the first term is the repulsive contribution, normally assumed as pairwise and described by a Born–Mayer type interaction, r_{ij} represents the distance between distinct gold atoms, and r_0 is the first-neighbors distance in a perfect crystalline lattice. The band contribution (second term) ensures system stability and is an attractive interaction (SMA) quantum mechanical in origin that incorporates many-body summations. The parameters D_1 , D_2 , p , q , and r_0 can be obtained using a simplistic algorithm with experimental values for cohesive energy, lattice parameters, and independent elastic constants for pure systems.

In this study, the physical stress that generates the NWs is simulated through structural change dimensions (increasing the distance between the outmost NW layers, for instance). We have considered different elongation rate variations, different temperatures, and initial velocity distributions. The temperature of the system is kept constant during each simulation using rescaling velocity scheme.³⁵ We use a Beeman algorithm³⁵ to integrate the equations of motion, with a time step of 2×10^{-15} s for all simulations. Our methodology does not use (in contrast with most of the previous work reported in the literature) periodic boundary conditions. This allows a more effective way to contrast experimental and theoretical data. The use of TB–SMA potentials makes our code exceptionally fast, requiring typically only 1–2 h in a Pentium IV setup for each simulated configuration.

To simulate the statistical aspects of experimental conditions, we use a random generator for the initial velocity distributions. Due to our low-cost computational simulations, we can generate many configurations to produce reliable statistical data of geometrical and other dynamical aspects, for example, associated with crystallographic orientations. In this way, the obtained results can be directly compared with experimental data. Also, we can apply external torsion in a controllable way to mimic internal stress. This makes the present methodology a very effective tool in the study of metallic NWs generated by mechanical elongation.

As shown in Figure 2, different crystallographic orientations produce structurally different NWs. To analyze the influence of the apex crystal orientation on the NW stability and dynamical elongation behavior, we have carried out molecular dynamics simulations for gold NWs along the [100], [111], and [110] axes. The initial geometric configuration of atoms is generated as a regular lattice for each crystallographic direction. To mimic the influence of the apex crystal orientation on the NW stability and dynamical growth, initial and end wire layers (two for [100] and [110], and

three for [111]) are kept geometrically constrained during simulations to induce a NW/apex epitaxial relation. These layers are free to move only along the NW elongation direction, but there are no constraints for the remaining layers. The temperature of the system is kept constant until the system achieves total energy equilibration, then we start to pull the wire along the NW growth direction. In our simulations we have considered temperatures varying from 300 up to 350 K, with typical elongation rates from 1 up to 5 m/s, and initial particle velocities randomly generated for each temperature value.

In Figure 3, we indicate some representative snapshots from the molecular dynamics simulations (see videos 6–8, Supporting Information) of the initial conditions (Figures 3a1, 3b1, and 3c1) passing through intermediate stages (Figures 3a2, 3b2, and 3c2) up to the LACs formation (Figures 3c3, 3b3, and 3c3). These simulations reveal two different and clear tendencies: formation of faceted pyramidal apices for [100] and [111] NWs (ex. upper apex in Figure 3b3) and appearance of elongated structures (rod-like) for [110] (ex. Figure 3c2). In fact, these behaviors reproduce the NW structural evolution experimentally observed by us and Ohnishi et al.,⁵ where well-faceted defect-free crystalline apices and wires are always generated during room temperature elongation processes (Figure 2). This is the first time that the dependence of NW morphology on crystal orientation was theoretically obtained.

From the simulations, we have obtained that LACs are formed for all three crystallographic orientations, with the number of gold atoms varying from 1 up to 8. These results are in good agreement with experimental data.^{5,8,12,13} In our simulations 55/60, 50/60 and 6/40 (X/Y where X is LAC formation event and Y is total number of simulations) LAC structures were observed for NWs generated along [111], [100], and [110] directions, respectively, with the following simulation conditions: [111] 240 ($4 \times 4 \times 15$) gold atoms, root-mean-square (rms) temperature 309 K, elongation rate 1 m/s; [100] 256 ($4 \times 4 \times 16$) gold atoms, rms temperature 310 K, elongation rate 1 m/s; and [110] 400 ($5 \times 5 \times 16$) gold atoms, rms temperature 308 K, elongation rate 1 m/s. These results show a clear tendency of statistical LAC occurrence decreasing from the [111], [100], to [110] axis. Our TB–SMA simulations are again in very good agreement with the experimental data⁸ where ductile (for [100] and [111] orientations) and brittle (for [110] orientation) behaviors have been observed (Figure 2 and videos 3–5, SI). The brittle behavior of [110] NWs can explain the low formation rate of LAC along this orientation. Although we have not observed any LAC formation along [110] axis in our HRTEM experiments, this has been reported by Onishi et al.⁵ The quick rupture of rod-like [110] wires may render difficult the detection of LAC formation within the time resolution of dynamic HRTEM measurements. Additional experimental evidence for the formation of LACs along [110] can be deduced from electrical transport experiments, where the conductance evolution of [110] NWs seldom shows very small shoulders or conductance plateaus at one quantum of conductance, indicating the formation of one-atom-thick

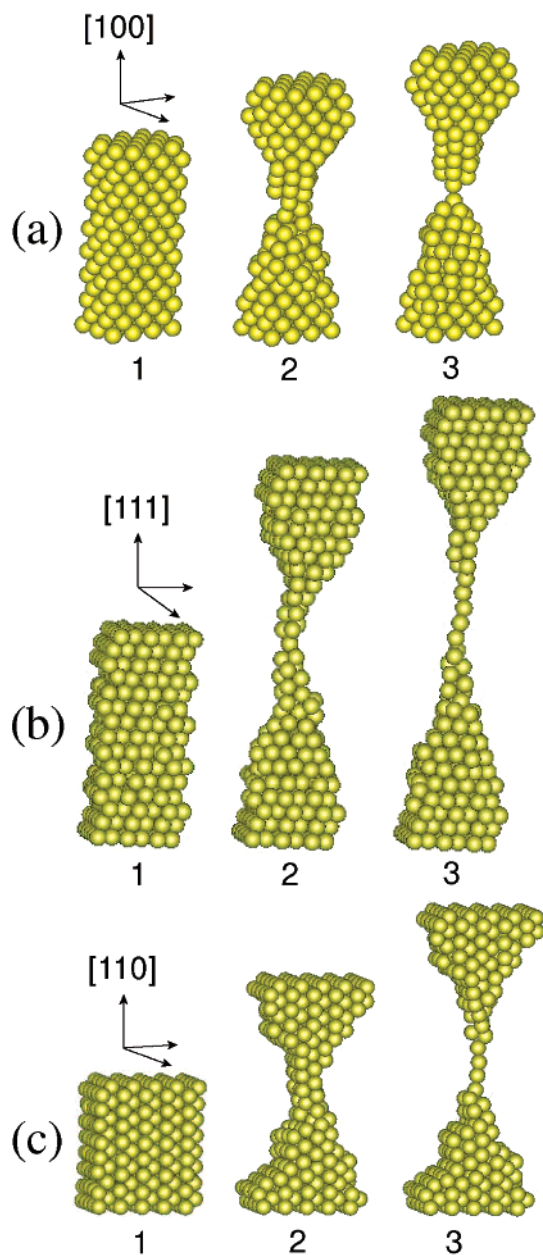


Figure 3. Representative snapshots from the molecular dynamics simulations showing the NW time evolution for different crystallographic orientations. See Figure 2 for comparison. The simulation conditions are: (a) 256 ($4 \times 4 \times 16$) gold atoms, root-mean-square (rms) temperature 309 K, elongation rate 1 m/s; (b) 240 ($4 \times 4 \times 15$) gold atoms, rms temperature 310 K, elongation rate 1.5 m/s; and (c) 400 ($5 \times 5 \times 16$) gold atoms, rms temperature 311 K, elongation rate 1 m/s.

contact or probably LACs with rather short lifetime (see Figure 3 in Rodrigues et al.⁸).

Several atomistic aspects of the NW formation can be derived from a thorough analysis of the simulations. For example, there is a large stabilization (~ 45 meV/atom) in an initial perfect fcc arrangement when compared with an imperfect arrangement, in agreement with HRTEM observations.^{8,23,29} The results pointed out that the formation of stacking faults in the nanometric constriction has a critical importance to render LAC formation less difficult. The observed critical importance of layer stacking has never been

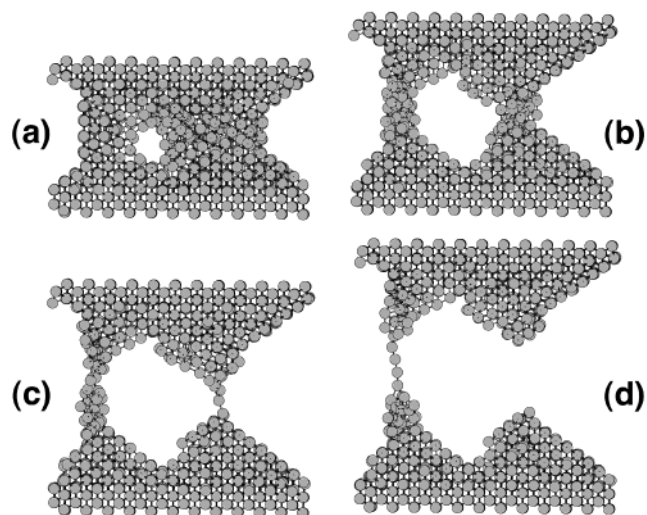


Figure 4. Representative snapshots sequence showing the time evolution of parallel columnar NW and LAC formation along the [110] orientation. The initial configuration is similar to those shown in Figure 3c1 and contains 1800 atoms (see video 10, Supporting Information). The simulation conditions are: 1800 ($10 \times 12 \times 15$) gold atoms, root-mean-square temperature 320 K, elongation rate 2 m/s.

addressed before in the literature, and it can explain part of the fluctuations in the experimental data, where it is not always possible to control the relative crystallographic orientation of NW apices. Another result is the confirmation of the importance of the slipping planes^{4,16} (see video 9, SI) to relieve the tensile stress and decrease the structural disorder. The balance between these two factors controls the formation of LACs. Finally, just before breaking, typical mean forces acting on gold atoms forming the LACs are in the range of 0.5–1.5 nN, in excellent agreement with experimental evidence.²⁴

Another interesting result from the simulations is that when we increase the aspect ratio of the structures we observed new dynamical features, such as the appearance of parallel columnar NWs (Figure 4). These structures present distinct behavior for the LAC evolution in terms of breaking regions and number of atoms (see video 10, SI). These results are the first theoretical observations of a process proposed by Marqu  ez and Garc  a³⁶, where nanowires could be formed as a result of multiple filaments or threads stretching. Although in our HRTEM experiments this behavior is unlikely to occur due to the NW fabrication procedures (thinning a bridge between two growing holes), it is a real possibility in mechanically controllable break junction experiments. The presence of such structures could explain the statistical fluctuations that are ever present in conductance data reported in the literature and deserve further investigation.

The low computational cost of our methodology has allowed the simulations of a large number (hundreds) of possible configurations at different initial conditions. With this information it was possible to elucidate the relationship between the stochastic nature of the experimental data and the theoretically derived structural features. The exceptional agreement we obtained with the experimental data reproducing the importance of the different crystallographic directions,

NW morphology, forces, stochastic fluctuations, etc., strongly points out that the kinetic aspects during NW elongation are the most important. Our simulations have showed that temperature values and elongation rates strongly affect the morphology and chance of NW formation. The temperature range and elongation rate we used were estimated to be consistent with the available experimental data. However, to have a better evaluation of the importance of these aspects, more detailed and comparative studies for different metals are necessary. Work along these lines are in progress. Further evidence of the robustness of the present methodology is revealed by the fact that predicted structures for NWs along the [111] axis have been applied to understand the correlation between atomic structure and the experimentally observed conductance behavior.²³

The methodology is completely general and can be used for any metallic fcc structure; it had produced reliable results and can be a very effective tool in the study of MNs and clusters. Work for Ag, Pt, Pd, Cu, Al, Pb, and Ni is in progress.

Acknowledgment. The authors thank the Brazilian Agencies CNPq, FAPESP, FAPEMIG, CAPES and Institutos do Milênio de Nanociências e Materiais Poliméricos – MCT.

Supporting Information Available: Related slideshow and videos. This material is available free of charge via the Internet at <http://pubs.acs.org>.

References

- (1) Agraït, N.; Yeyati, A. L.; van Ruitenbeek, J. M. *Phys. Rep.* **2003**, 377, 81.
- (2) Landman, U.; Luedtke, W. D.; Burnham, N. A.; Colton, R. J. *Science* **1990**, 248, 454.
- (3) Krans, J. M.; van Ruitenbeek, J. M.; Fisun, V. V.; Yanson, I. K.; de Jongh, L. J. *Nature (London)* **1995**, 375, 767.
- (4) Landman, U.; Luedtke, W. D.; Salisbury, B. E.; Whetten, R. L. *Phys. Rev. Lett.* **1996**, 77, 1362.
- (5) Ohnishi, H.; Kondo, Y.; Takayanagi, K. *Nature (London)* **1998**, 395, 780.
- (6) Yanson, A. I.; Rubio Bollinger, G.; van den Brom, H. E.; Agraït, N.; van Ruitenbeek, J. M. *Nature (London)* **1998**, 395, 783.
- (7) Sánchez-Portal, D.; Artacho, E.; Junquera, J.; Ordejón, P.; García, A.; Soler, J. M. *Phys. Rev. Lett.* **1999**, 83, 3884.
- (8) Rodrigues, V.; Fuhrer, T.; Ugarte, D. *Phys. Rev. Lett.* **2000**, 85, 4124.
- (9) Muller, C. J.; van Ruitenbeek, J. M.; de Jongh, L. J. *Physica (Amsterdam)* **1992**, 191C, 485.
- (10) Kondo, Y.; Takayanagi, K. *Phys. Rev. Lett.* **1997**, 79, 3455.
- (11) Kizuka, T. *Phys. Rev. Lett.* **1998**, 81, 4448.
- (12) Rodrigues, V.; Ugarte, D. *Phys. Rev. B* **2001**, 63, 073405.
- (13) Kizuka, T.; Umehaa, S.; Fujisawa, S. *Jpn. J. Appl. Phys.* **2001**, 240, L71.
- (14) Koizumi, H.; Oshima, Y.; Kondo, Y.; Takayanagi, K. *Ultramicroscopy* **2001**, 88, 17.
- (15) Todorov, T. N.; Sutton, A. P. *Phys. Rev. Lett.* **1993**, 70, 2138.
- (16) Sorensen, M. R.; Brandbyge M.; Jacobsen, W. *Phys. Rev. B* **1998**, 57, 3283.
- (17) da Silva, E. Z.; da Silva, A. J. R.; Fazzio, A. *Phys. Rev. Lett.* **2001**, 87, 256102.
- (18) Kang, J. W.; Hwang, H. J. *Nanotechnol.* **2002**, 13, 503.
- (19) Stafford, C. A.; Baeriswyl, D.; Bürki, J. *Phys. Rev. Lett.* **1997**, 79, 2863.
- (20) Yannouleas, C.; Landman, U. *J. Phys. Chem. B* **1997**, 101, 5780.
- (21) Lang, N. D. *Phys. Rev. Lett.* **1997**, 79, 1357.
- (22) Wan, C. C.; Mozos, José-Luiz; Taraschi, G.; Wang, J.; Go, H. *Appl. Phys. Lett.* **1997**, 71, 419.
- (23) Rego, L. G. C.; Rocha, A. R.; Rodrigues, V.; Ugarte, D. *Phys. Rev. B* **2003**, 67, 045412.
- (24) Rubio-Bollinger, G.; Bahn, S. R.; Agrait, N.; Jacobsen, K. W.; Vieira, S. *Phys. Rev. Lett.* **2001**, 87, 026101.
- (25) Barnet, R. N.; Landman, U. *Nature (London)* **1997**, 87, 788.
- (26) Nakamura, A.; Brandbyge, M.; Hansen, L. B.; Jacobsen, K. W. *Phys. Rev. Lett.* **1999**, 82, 1538.
- (27) Legoas, S. B.; Galvão, D. S.; Rodrigues, V.; Ugarte, D. *Phys. Rev. Lett.* **2002**, 88, 076105.
- (28) Kruger, D.; Fuchs, H.; Rousseau, R.; Marx, D.; Parrinello, M. *Phys. Rev. Lett.* **2002**, 89, 186402.
- (29) Rodrigues, V.; Bettini, J.; Rocha, A. R.; Rego, L. G. C.; Ugarte, D. *Phys. Rev. B* **2002**, 65, 153402.
- (30) Cleri, F.; Rosato, V. *Phys. Rev. B* **1993**, 48, 22.
- (31) Tománek, D.; Aligia, A. A.; Balseiro, C. A. *Phys. Rev. B* **1985**, 32, 5051.
- (32) Ducastelle, F. *J. Phys. (Paris)* **1970**, 31, 1055.
- (33) Cleri, F.; Mazzone, G.; Rosato, V. *Phys. Rev. B* **1993**, 47, 14541.
- (34) Evangelakis, G. A.; Kallinteris, G. C.; Papanicolaou, N. I. *Surf. Sci.* **1997**, 394, 185.
- (35) Allen, M. P.; Tildesley, D. J. *Computer Simulation of Liquids*; Oxford University Press: Oxford, 1996.
- (36) Correia, A.; Marquéz, M. I.; García, N. In *Nanowires*; Serena, P. A., García, N., Eds.; NATO ASI Series, Series E: Applied Sciences; Kluwer Academic Publishers: The Netherlands, 1997; Vol. 340, pp 311–325.

NL049725H